Investigation of Silica Gels as Adsorbents in SO_2 Enriched Gases

F. Klenert, S. Thiel, C. G. Aneziris, S. Krzack

Flue gas cleaning in power plants is required to remove harmful components such as sulphur dioxide SO_2, mercury Hg, nitrogen oxides NO_x, volatile organic compounds VOC, hydrochloric acid HCl, hydrogen fluoride HF, heavy metals, dioxins, furans and fly ash. In this study, the adsorption performance of silica gels, the breakthrough behaviour regarding SO_2 rich gases and the regeneration of silica gels were investigated. Firstly, the influence of different grain sizes on the adsorption of SO_2 and secondly the ability of regeneration regarding different grain sizes and relative humidity of storing the silica gels were examined. The best silica gel achieved 25 % of dynamic adsorption capacity and 72 % of the breakthrough time compared to active coke. Suitable conditions for complete thermal regeneration of silica gels were found. Dependent on the grain size and relative humidity of storing the silica gels, a coarse grain and medium relative humidity of 45 % was favourable for a complete regeneration.

1 Introduction

Flue gas cleaning has received much attention due to the aspired environmental protection. The most frequently occurring pollutants are nitrogen oxides (NO_x), sulphur dioxides (SO_x), organic substances, halogen compounds and heavy metals (Hg) [1, 2]. Besides filters and selective catalytic reduction techniques, different materials are used to clean flue gases such as carbonaceous adsorbents (activated carbon, active coke), mineral adsorbents (zeolites), trass and combined materials [3].

Liberti et al. [4] investigated urban particulate matter from the atmosphere as well as fly ash from oil and coal electric power furnaces, from a cement factory or from iron and steel plants. They found that SO_2 is adsorbed on the surface of several particles, which is strongly influenced by humidity. Also DeBarr et al. [5], Daley et al. [6], Rodriguez-Mirasol et al. [7] and Kisamori et al. [8] investigated carbonaceous adsorbents such as activated carbons and activated carbon fibers (ACFs). DeBarr et al. [5] found out that both materials are beneficial as sorbents with a large capacity for SO_2. Daley et al. [6] and Kisamori et al. [8] confirmed the possibility of ACFs and Rodriguez-Mirasol et al. [7] of activated carbons to adsorb SO_2. Krzack [9], Heschel et al. [10] and Krzack et al. [11] investigated active cokes for flue gas cleaning.

Cole et al. [12] investigated ion exchange resins in the chloride form and molecular sieves to recover sulphur dioxide from waste gas. They found that ion exchange resins show adsorption capacities similar to activated charcoal. Sirkecioglu et al. [13] investigated clinoptilolite, a silica rich natural zeolite, to remove H_2S and SO_2 from natural gas, air and hydrocarbon gas streams. They spotted the adsorption capacity for SO_2 to be higher than for H_2S due to its higher permanent dipole moment. Also Tantet et al. [14] confirmed that hydrophobic zeolites could adsorb SO_2. They found that in the presence of water the adsorption of SO_2 is declined. Belyakova et al. [15] investigated the adsorption of SO_2 and CO_2 on silica gels with amines as functional groups. They figured out that the amount of adsorbed SO_2 is dependent on the surface concentration of amino groups. In addition, Thornsberry [16] confirmed that silica gels could be used as gas chromatographic separation materials for SO_2. Furthermore, Ahmed et al. [17] investigated aerogels containing components such as CaO and MgO in their structure to adsorb SO_2.

A combined material was investigated by Zhao et al. [18] as they supported ether-functionalized imidazolium-based ionic liquids (EFILLs) onto porous silica gel particles by an impregnation method. By this material, a high SO_2 adsorption rate can be achieved.

To date, various materials were investigated regarding the adsorption of SO_2 in flue gases. However, little attention has been paid to desorption of SO_2 for regeneration of the adsorbent materials, especially pure silica gels. It is known that carbon adsorbents can be regenerated [19, 20], but the regeneration process is associated with exorbitant effort since a specific residual load-

Friederike Klenert, Christos G. Aneziris
Institute of Ceramic, Glass and Construction Materials, TU Bergakademie Freiberg
Freiberg
Germany

Stefan Thiel, Steffen Krzack
Institute of Energy Process Engineering and Chemical Engineering,
TU Bergakademie Freiberg
Freiberg
Germany

Corresponding author: *Friederike Klenert*
E-mail: friederike.klenert@ikgb.tu-freiberg.de

Keywords: adsorption of SO_2, desorption of SO_2, regeneration of adsorbents, flue gas treatment, silica gel

Received: 12.12.2016
Accepted: 22.12.2016

ing occurs [20]. Furthermore, the carbon surface reacts during an oxidative thermal treatment with the oxygen and leads to the formation of CO and CO_2 [19]. Due to the expensive treatment, only high performance activated carbons are regenerated, whereas most carbon based sorbents are designed as one-way products. In contrast, it is known that silica gels adsorbed with sulphurous components, such as H_2S, can be regenerated [21, 22]. In this study, the adsorption performance, the breakthrough behaviour of silica gels regarding SO_2 rich gases and the regeneration of silica gels were investigated. Firstly, the influence of different grain sizes on the adsorption of SO_2 and secondly the ability of regeneration regarding different grain size and relative humidity of storing the silica gels was examined.

2 Experimental

This research work investigated the adsorption and desorption of sulphur dioxide (SO_2) on silica gels as new adsorbent in comparison with a commercial active coke. The material was characterized by the porosity P, average pore radius r, microscopic measurements and differential scanning calorimetry. The adsorption/desorption was distinguished by breakthrough curves and the silica gels dynamic adsorption capacity and the breakthrough time.

2.1 Materials

In recent studies from Klenert et al. [23, 24] silica gels as transparent heat insulation applications were investigated. Based on the results, an assortment of silica gels was chosen to investigate the SO_2 adsorption behaviour. To exclude property fluctuations of silica gels, an industrial silica gel with related properties named silica gel C, produced by Chemiewerk Bad Köstritz GmbH (Bad Köstritz/DE) was used for the studies. Samples of the initial material were dried at 50 °C, 100 °C and 150 °C for 30 min to remove physically adsorbed water before adsorption experiments. Simultaneously, commercial active coke HOK medium (RWE AG) was used as reference.

2.2 Analytical methods

Isotherms of low thermal adsorption (77 K) and desorption of nitrogen on the granular materials were measured (ASAP 2010, Micromeritics/DE) to analyze especially the micropores region (<2 nm). From the data obtained, the specific surface areas as well as the pore size distributions and the cumulative pore volume of the granular materials were determined. The Horwath Kawazoe method DIN 66135-4:2004-09 for analysis in micropores region was used. In mesopore region, the Barrett-Joyner-Halenda method (BJH) according to DIN 66134 for analyses in case of silica gels, and the BET method DIN ISO 9277 for HOK was used. The pore size distribution, the average pore radius and the cumulative pore volume in the meso- and macropores region of the materials was determined with a mercury porosimeter (PASCAL 140/440, Porotec GmbH/DE). Cumulative volume distributions were derived according to the standard DIN 66133/ISO 15901-1. To calculate the porosity of the materials, the true density was firstly investigated with a helium pycnometer (Accupyc 1330, Micromeritics GmbH/DE) in compliance with DIN 66137-2. The porosity P is associated with the true density ρ_t and the cumulative pore volume V_{cum} according to equation 1:

$$P = \frac{V_{cum}}{\frac{1}{\rho_t} + V_{cum}} \qquad [1]$$

The microstructure of the silica gels was investigated by scanning electron microscopy (SEM). For the SEM investigations (XL30ESEM-FEG, FEI/DE), the silica gels were dried at 150 °C, a number of grains were arranged on an object plate and then carbon sputtered.

Furthermore, differential scanning calorimetry and thermogravimetric measurements (STA 409 PC/PG, Netzsch/DE) were used to characterize the behaviour of the material at elevated temperatures and to determine the maximum application temperature. The heating-up rate was 10 K/min and the DSC/TG measurements were performed in synthetic air atmosphere with mostly 80 % N_2 and 20 % O_2. Different heat flows between the sample and reference were measured and, due to exothermal or endothermal reactions, various physical transformations were characterized [25]. Additionally, the change of the silica gels mass due to reactions while heating were determined.

SO_2 adsorption was performed in a heated fixed bed reactor coupled with a downstream online SO_2 analyser (Ultramat Z23, Siemens/DE). The sorption tube consists of glass with a maximum bed diameter of 31 mm and a maximum bed height of 58 mm. Prior to adsorption, the silica gels were heated up to 150 °C for 30 min in a drying oven and were then filled in the glass tube with an average bed height of 20 mm. The reactor was heated up to 120 °C bed temperature for 1 h. After 40 min, the gas mixture of 32 l/h synthetic air (79 vol.-% N_2 and 21 vol.-% O_2) and 3 l/h of SO_2 (0,4 vol.-%, N_2 as residual gas) was lead into the aperture, streaming around the reactor in bypass until a constant gas flow and concentration of SO_2 was achieved after 20 min. Starting the adsorption investigation, the gas flow with 350–370 ppm SO_2 was introduced into the reactor for 30 min, passing through the bed from the top. Afterwards the heating was

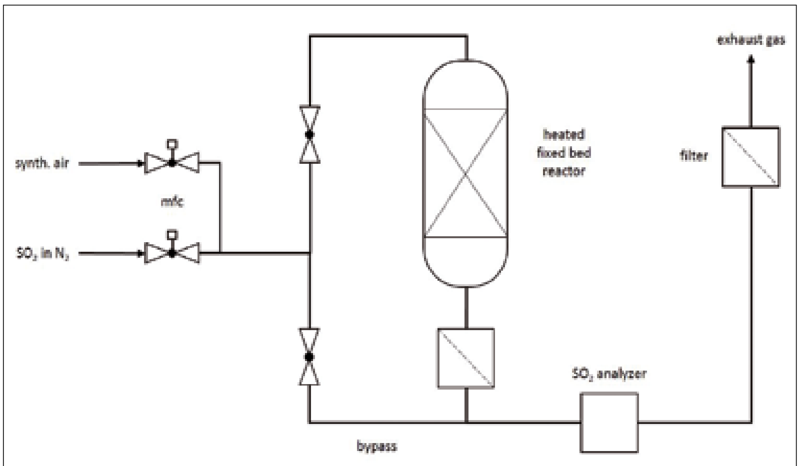

Fig. 1 Experimental set up of SO_2 breakthrough curve measurements

switched off and the inlet concentrations c_0 were measured again to avoid drift bias. The logged values for time-dependent SO_2 concentrations were used to visualize the breakthrough curves and calculate specific values such as breakthrough time (achieving $c/c_0 > 0,1$), breakthrough capacity and dynamic adsorption capacity ($c/c_0 = 0,6$).
The mass change due to adsorption of SO_2 on the sorbent was calculated by

$$\Delta m_{SO_2} = \frac{\eta_{SO_2}}{100\ \%} \cdot c_{SO_2} \cdot \dot{V} \cdot 10^{-3} \cdot \frac{t}{60 \frac{min}{h}} \quad [2]$$

and the dynamic load capacity of the sorbent x_1 by

$$x_1 = \frac{\Delta m_{SO_2}}{m_0} \quad [3]$$

The regeneration of the sorbent was performed in a separate drying oven. The sorbent was heated up to 250 °C for 5 h in oxidizing atmosphere. Afterwards, the regenerated sorbents were tested again for their adsorption behaviour regarding breakthrough curve and dynamic adsorption capacity of the sorbent. The level of regeneration was calculated by

$$R = \frac{x_{dyn\,2}}{x_{dyn\,1}} \quad [4]$$

$X_{dyn,\,1}$ = dynamic adsorption capacity of first adsorption
$X_{dyn,\,2}$ = dynamic adsorption capacity of second adsorption (after regeneration).

3. Results and discussion

3.1 Production of different grain size distributions of silica gels

In preliminary investigations, silica gel V1 as a promising material for SO_2 adsorption was ascertained. Based on the results, systematic investigations of silica gels regarding the adsorption of SO_2 were conducted. V1 was a statistic mixing, which was tested as it was produced. For adsorption measurements, three silica gels ($V2/V2_{reg.}$, $V3/V3_{reg.}$ and $V4/V4_{reg.}$) with different grain sizes were produced and compared with HOK medium as a standard material, as seen in Fig. 2.
Silica gels V2, V3 and V4 were first loaded with SO_2 and then regenerated. The regenerated silica gels $V2_{reg.}$, $V3_{reg.}$ and $V4_{reg.}$ correspond to V2, V3 and V4 and are identical with the material and porosity structure.

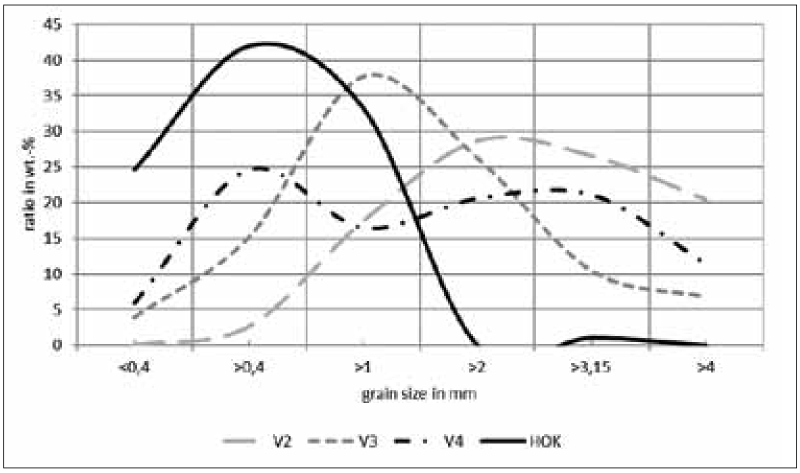

Fig. 2 Grain size distribution of different silica gels and HOK medium

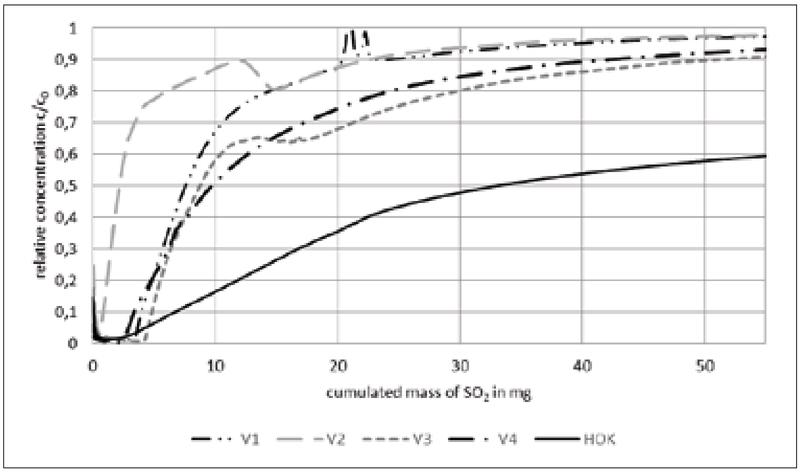

Fig. 3 SO_2 concentration of silica gels V1–V4 and HOK over time

HOK medium exhibited a narrow grain size distribution with grains smaller than 2 mm, especially with mostly 0,4 mm in diameter. All silica gels are characterized by a broader grain size distribution compared to HOK medium and larger grains. Silica gel $V2/V2_{reg.}$ is mostly characterized by grains larger than 2 mm in diameter and presents a coarse grain. Contrary, silica gel $V3/V3_{reg.}$ exhibited fine grains mostly with smaller grains of 1 mm. $V4/V4_{reg.}$ represented a bimodal grain size distribution with grains mostly between 0,4–1 mm and 2–3 mm. These different silica gels are investigated regarding the adsorption and desorption behaviour.

3.2 Adsorption behaviour of SO_2 on silica gels and carbonaceous adsorbents

Different silica gels V1, V2 and V3 as well as HOK medium were investigated regarding the breakthrough curve of SO_2 and the course of pressure during the adsorption. Fig. 3 shows the trends of the relative concentration c/c_0 for all five materials.
Silica gel V2 showed the earliest breakthrough with 0,8 mg SO_2 loaded until breakthrough, whereas the silica gels V1 (1,9 mg), V4 (3,4 mg) and V3 (4,9 mg) exhibited larger values. After 90 min adsorption, nearly the initial SO_2 concentration was achieved for every silica gel. Contrary, HOK medium showed a very low rise of the breakthrough curve with a large breakthrough time with 13,2 mg SO_2 loaded.
The discontinuity of the silica gel breakthrough curves can be traced back to the properties of the filling. At silica gel V1, the discontinuity appeared at 20–23 mg SO_2 loaded, for V2 at 12–15 mg SO_2 loaded, for V3 at 13–15 mg SO_2 loaded and V4 at 5–7 mg SO_2 loaded (Fig. 3). Contrary, HOK medium showed a very constant SO_2

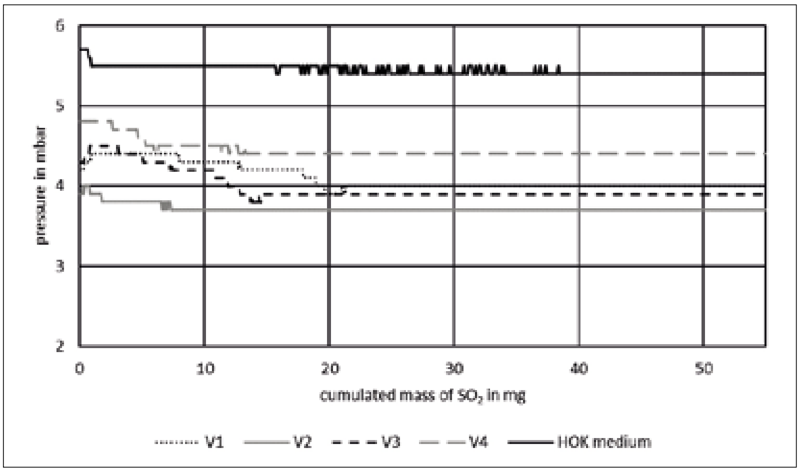

Fig. 4 Pressure over different fillings

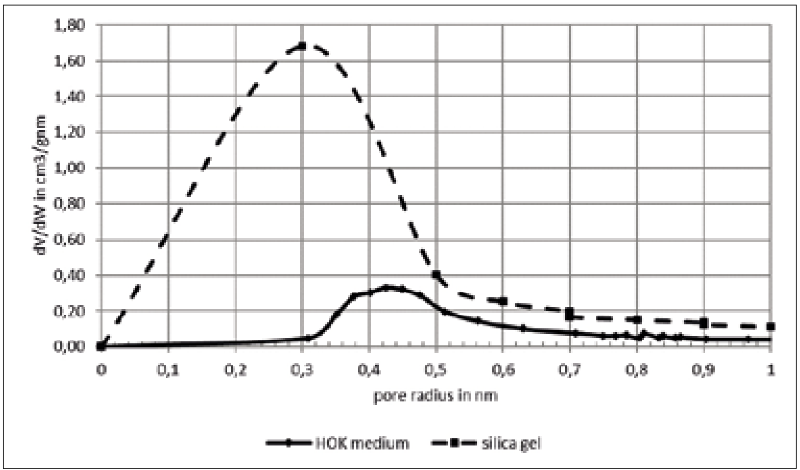

Fig. 5 Pore size distribution by nitrogen adsorption measurements of HOK medium and silica gel

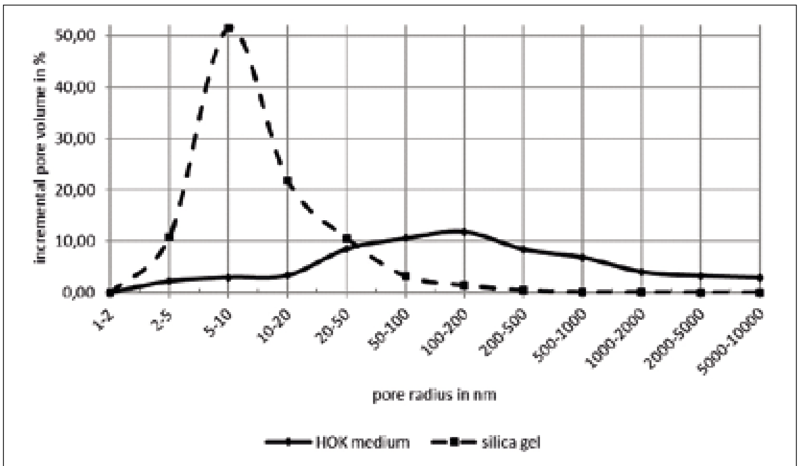

Fig. 6 Pore size distribution by mercury intrusion measurements of HOK medium and silica gel

adsorption behaviour without almost any discontinuity. Although the absolute pressure at 5,5 mbar in maximum is small, the course of pressure seemed to have an influence on the adsorption behaviour. With a constant pressure behaviour on the filling, a constant curve progression could be achieved (Fig. 4). Every silica gel showed a discontinuity of the curve progression about that time the pressure drop took place. This pressure drop seemed to appear especially for the silica gel V3 with the highest fine grain content. This discontinuity suggests to not optimal grain size distributions leading to irregular streaming in different grain heights. This can be verified by Sonnenburg [26] and Klöker et al. [27] as they concluded that in fillings local velocity maxima do exist and the streaming is not uniform.

The more efficient adsorption behaviour of HOK medium deduced from many aspects, especially the narrow grain size distribution with mostly fine particles at 0,4 mm (Fig. 2) and the optimal streaming behaviour of HOK medium (Fig. 4).

The influence of particle size on adsorption behaviour was investigated by Karau et al. [28] and Yean et al. as they confirmed that fine particles could increase the breakthrough time. This mechanism can be explained by the shortened diffusion path length without a high mass transfer resistance within the adsorbent particles [29]. Rasmuson [30] found a delay of the breakthrough point and faster reached adsorption equilibrium by using smaller particles.

The pore size distribution of a typical silica gel and HOK medium in the micropores region is represented in Fig. 5, whereas Fig. 6 shows the meso- and macropores region of the materials. It is assumed that the pore size distribution of the silica gels V1, V2 and V3 and V4 is similar since only the grain size distribution was changed.

The pore size distribution of HOK medium was bimodal with pores in the micropores region, especially 0,4 nm and pores in the macropores region about 100 nm. HOK medium mostly consisted of 49 % micropores (<2 nm) and 42 % macropores (>50 nm) with a BET surface of 267 m^2g^{-1} and 55 % porosity. Contrary, the silica gel showed a bimodal pore size distribution, with a larger micropores ratio at 0,3 nm and meso pores at 5–10 nm. Almost no macropores were existent. The silica gel mostly possessed of 50 % meso pores (2 nm < pore size < 50 nm) with a BJH surface area of 446 m^2g^{-1} and 54 % porosity. Especially in micropores adsorption mechanisms take place, whereas meso and macropores serve as gas transport pathways [31]. Therefore, HOK medium is advantageous to pass gases fast from the outside to the inner surfaces.

From Fig. 7, the surface structure of HOK medium (A) and silica gel (B) could be determined. HOK medium exhibited a much coarser structure with bigger particles. Contrary, the silica gel showed a more even structure. As Iler [32] investigated, silica gels consist of an aggregation and polymerization of particles in a three-dimensional Si–O–Si microstructure.

In atmospheres with water vapour, HOK medium acts as a catalyst and converts SO_2 with O_2 to SO_3 and reacts with H_2O to H_2SO_4, which is described by Tseng et al. [33] and Kast [34] with

$$SO_2 + \frac{1}{2}O_2 \rightarrow SO_3 \quad [5]$$

$$SO_3 + H_2O \rightarrow H_2SO_4 \quad [6]$$

However, in the adsorption experiments the SO_2/N_2 gas stream was not enriched with H_2O vapour and thus especially SO_3 was generated at HOK medium. Although in the test gas a dry gas atmosphere was existent, silica gels can build SO_3 and H_2SO_4 as in the reactions [5] and [6] (presented in Fig. 8–9). The unloaded silica gel showed a distinctive endothermic peak at approx. 90 °C due to the evaporation of adsorbed water on the pore surfaces. With increasing temperatures (100–700 °C), a broad exothermic hump was existent and can be traced back to the condensation and densification process of silanol groups to siloxane groups, in which water molecules are produced [35, 36]. The curve progression of the loaded silica gel was completely different with no endothermic peak but a plateau at the temperature range 35–60 °C and a broad but more intensive exothermic hump from 100–700 °C. The maximum of exothermic hump was existent at the same temperature at 450 °C for both silica gels but the rise of the loaded silica gel was steeper than for the unloaded silica gel. Based on these results, it can be concluded that firstly, in the adsorption process at 120 °C water molecules are built by condensation of silanol groups to siloxanes, which can react with SO_3 to H_2SO_4. Secondly, at higher temperatures in the DSC/TG measurements, again water molecules are generated by condensation processes of silanols to siloxanes, which can form H_2SO_4. Therefore, the higher exothermic enthalpy is characteristic for the reactions [5] and [6] and the SO_2 is physically bonded on SiOH groups in a first step and is then converted with O_2 to SO_3 and reacts with H_2O to H_2SO_4. The thermogravimetric measurements showed, that the unloaded silica gel (11 mass-%) exhibited a stronger distinctive mass loss than the loaded silica gel (9 mass-%) but a parallel curve progression. The mass difference can be traced

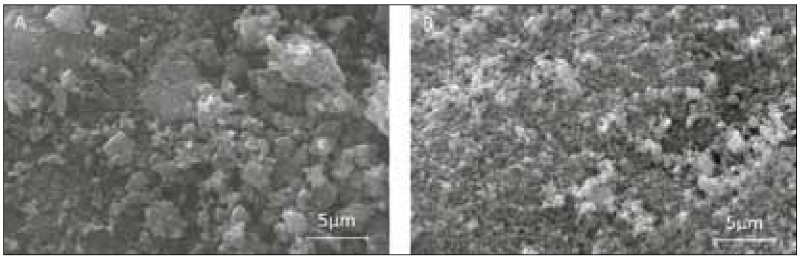

Fig. 7 Scanning electron microscopic images of A) HOK medium, and B) silica gel

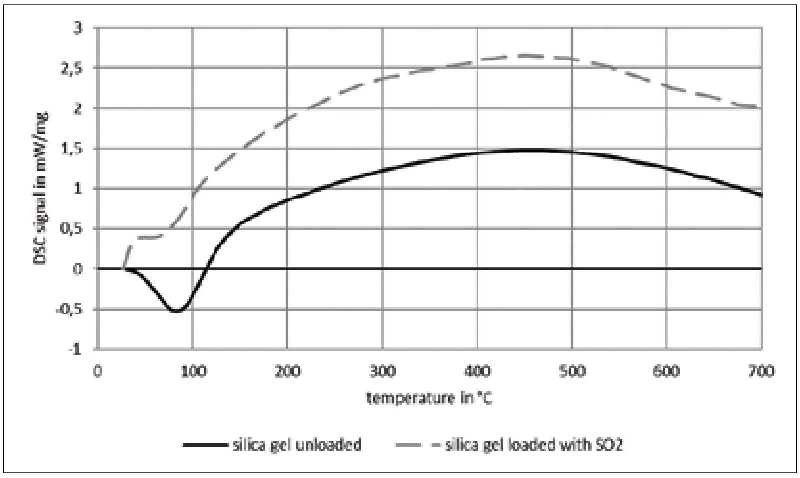

Fig. 8 Differential scanning calorimetric measurement of unloaded silica gel and silica gel loaded

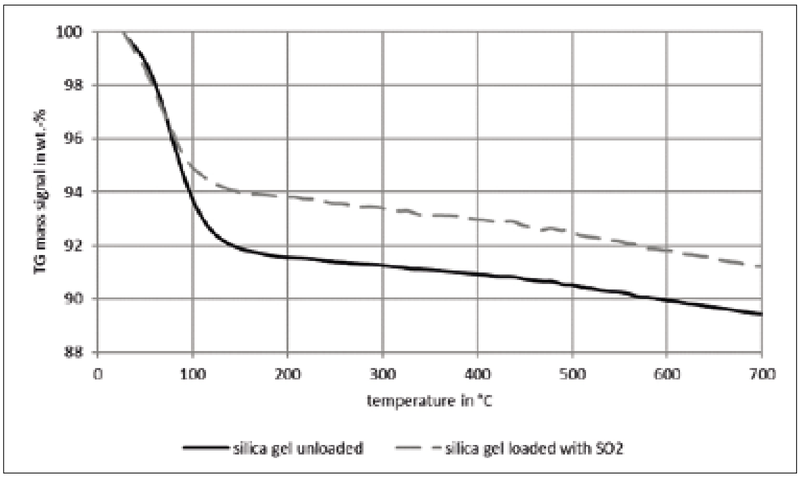

Fig. 9 Thermogravimetric measurement of unloaded silica gel and loaded silica gel

Tab. 1 Breakthrough time, dynamic breakthrough capacity and dynamic adsorption capacity of silica gels V1, V2, V3, V4, and HOK medium

Material	V1	V2	V3	V4	HOK Medium
Breakthrough Time [s/g]	48	9,8	25	17	67
Dynamic Breakthrough Capacity [mg/g]	0,5	0,1	0,3	0,2	0,7
Dynamic Adsorption Capacity (c/c_0 = 0,6) [mg/g]	1,1	0,3	0,6	0,7	4,4

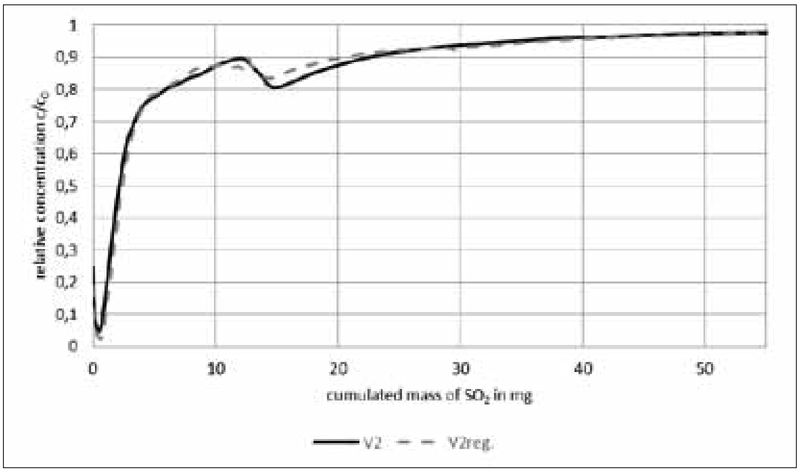

Fig. 10 First (V2) and second SO_2 adsorption ($V2_{reg.}$ after regeneration), 45 % relative humidity

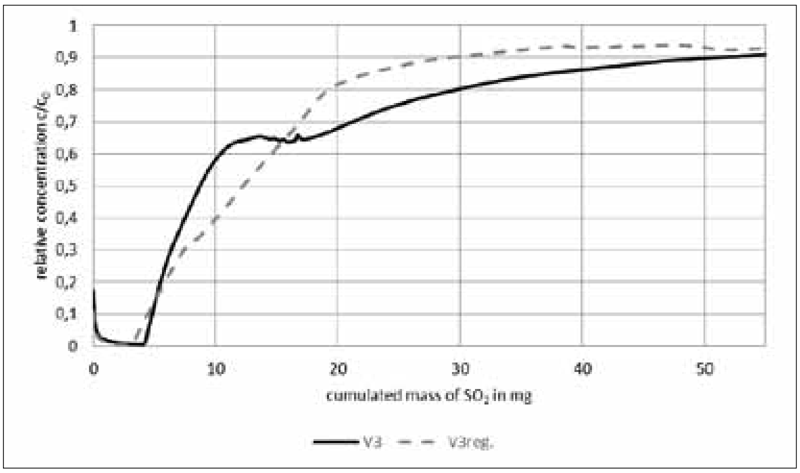

Fig. 11 First (V3) and second SO_2 adsorption ($V3_{reg.}$ after regeneration), 70 % relative humidity

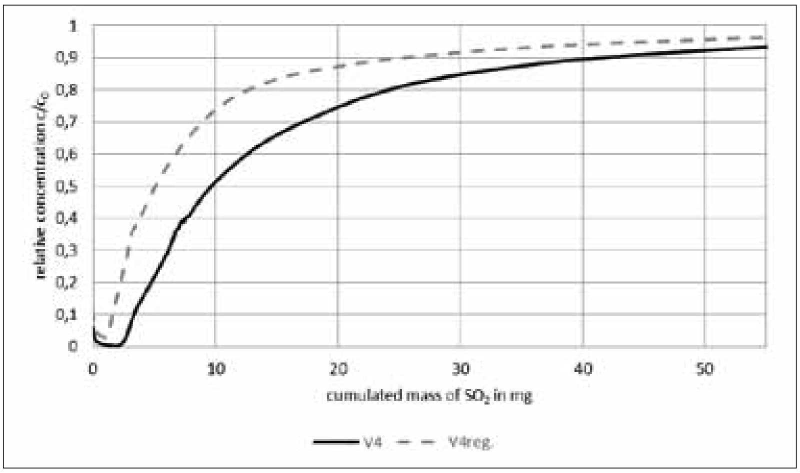

Fig. 12 First (V4) and second SO_2 adsorption ($V4_{reg.}$ after regeneration), 20 % relative humidity

back to the less water desorption <100 °C due to the loading with SO_2.

The adsorption performance (breakthrough time, dynamic breakthrough capacity and dynamic adsorption capacity) of different silica gels compared to HOK medium shown in Tab. 1. The dynamic breakthrough capacity is the amount of SO_2 adsorbed in the silica gels after breakthrough time, when the relative concentration exceeds c/c_0 = 0,1. However, to get a better comparison of different measured silica gels with low breakthrough times, the dynamic adsorption capacity is determined to be the adsorbed SO_2 mass at a relative concentration of c/c = 0,6.

The breakthrough time as well as the adsorption capacity can be increased with decreasing grain size. Therefore, V2 with a coarse grain of 2 mm exhibited the smallest breakthrough time (9,8 s/g), dynamic breakthrough capacity (0,1 mg/g) and adsorption capacity (0,3 mg/g) compared to V3 with 1 mm fine grains (25 s/g, 0,3 mg/g and 0,6 mg/g) and V1 with statistically mixed grains (48 s/g, 0,5 mg/g and 1,1 mg/g). V4 exhibited a similar dynamic breakthrough capacity of 0,2 mg/g due to its coarse grains of 3 mm. Karau et al. [28], Yean et al. [29] and Rasmuson [30] found out that decreasing particle sizes lead to shortened diffusion path lengths without a high mass transfer resistance within the adsorbent particles. Tsai et al. [37] confirmed as well that smaller particles enhance the adsorption rate and contribute to a larger length of the used bed than coarse particles. Furthermore, fine grains contribute to larger pressures over the adsorbent than coarse grains (Fig. 4). The statistic grains led to the best results, which can be explained by the optimal adsorption and streaming conditions with a high quantity of small particles. This can be verified by a high pressure over the filling compared to V2 and V3 (Fig. 4) and therefore a high mass transfer by shortened diffusion path length was reached. In fact, V4 exhibited the highest pressure but the bimodal grain size distribution led to disadvantageous streaming behaviour. Therefore, the best silica gel V1 achieved 25 % of dynamic adsorption capacity and 72 % of the breakthrough time compared to HOK medium.

3.3 Regeneration of silica gels

Besides the adsorption of silica gels, the regeneration of the granular materials was investigated. The granular materials were loaded in a first experiment with SO_2, dried at 250 °C for 5 h and stored at a relative humidity of 20–70 % for 10–18 days. The influence of the grain size distribution and relative humidity during the storage on the second adsorption of SO_2 on silica gels was investigated. The grain size distributions are analysed in 3.1. Each initial silica gel V2, V3, V4 exhibited exactly the same grain size distribution like their correspondent $V2_{reg.}$, $V3_{reg.}$, $V4_{reg.}$ since only the regeneration process differs from each other. In Fig. 10–12 the first adsorption as well as the second SO_2 adsorption (after regeneration) on silica gels V2, V3 and V4 is shown.

Silica gel $V2_{reg.}$ is the only silica gel, which could be regenerated completely with nearly identical breakthrough time and adsorption capacity like its correspondent V2 (Fig. 10) with 1,1 mg SO_2 loaded until breakthrough. Contrary, the silica gels $V3/V3_{reg.}$ (4,9 mg /4,5 mg) and $V4/V4_{reg.}$ (3,4 mg/1,7 mg) could not be regenerated completely with different breakthrough and adsorption behaviours. Therefore, silica gels $V3_{reg.}$ and $V4_{reg.}$ exhibited a steeper curve progression of adsorption with a rather saturation than their correspondent V3 and V4.

Furthermore, silica gel $V3_{reg.}$ with the highest fine grain content (Fig. 2) exhibited the highest pressure of 19 mbar as well as the largest pressure drop of 14 mbar over the filling (Fig. 13). Contrary, silica gel $V2_{reg.}$ with the largest grain size exhibited the smallest pressure of approx 3,7 mbar as well as the smallest pressure drop of 0,7 mbar. Silica gel $V4_{reg.}$ with both fine and coarse grain size showed a medium pressure of 4,4 mbar and a pressure drop of 0,4 mbar. Due to the smallest pressure drop at silica gel $V4_{reg.}$, the breakthrough curve was very uniform. The relation between grain size and pressure/pressure drop was found at the first loaded silica gels (chapter 3.2) and can be verified for regenerated silica gels as well.

In Tab. 2, the breakthrough time, the dynamic breakthrough capacity and dynamic adsorption capacity of silica gels $V2_{reg.}$, $V3_{reg.}$, $V4_{reg.}$ are shown. In comparison to the prior experiments, the breakthrough time of the regenerated silica gels declines except of $V2_{reg.}$. This is due to the circumstance that the residual loading after the regeneration treatment lowers the time until $c/c_0 = 0,1$ is achieved (especially $V4_{reg.}$) and the not uniform streaming behaviour (especially $V3_{reg.}$). Regarding to the breakthrough time and the dynamic breakthrough capacity and dynamic adsorption capacity, silica gel $V3_{reg.}$ exhibited the highest value of 21 s/g, 0,2 mg/g, 0,7 mg/g due to its small grain size of 1 mm (Fig. 2). Therefore, the small grain size generated, firstly, a larger pressure over the filling (Fig. 13) and secondly shortened diffusion path lengths than in cases for the silica gels $V2_{reg.}$ and $V4_{reg.}$ [28–30].

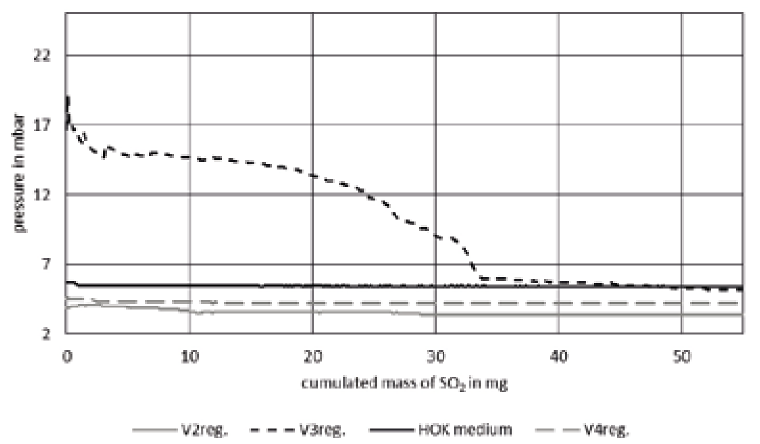

Fig. 13 Pressure over different regenerated fillings

Tab. 2 Breakthrough time, dynamic breakthrough capacity and dynamic adsorption capacity of silica gels $V2_{reg.}$, $V3_{reg.}$ and $V4_{reg.}$

Material	$V2_{reg.}$	$V3_{reg.}$	$V4_{reg.}$
Breakthrough Time [s/g]	14	21	8
Dynamic Breakthrough Capacity [mg/g]	0,1	0,2	0,09
Dynamic Adsorption Capacity (c/c_0 = 0,6) [mg/g]	0,4	0,7	0,4

However, V2 is the only silica gel which could be regenerated (compare Tab. 1 and Tab. 2). This fact can be reasoned by the different storage of silica gels after regeneration. Silica gel $V4_{reg.}$ was stored in a very dry atmosphere in 20 % relative humidity, whereas $V2_{reg.}$ was stored at 45 % and $V3_{reg.}$ in a very wet atmosphere with 70 % relative humidity. It seemed to be an optimum of storage conditions in a medium relative humidity atmosphere. Mehlhorn et al. [38], Lincke et al. [39] and Ramesohl et al. [40] found out that a certain water film on the surface of iron materials is advantageous for adsorption.

Therefore, there is likely a similar relation between relative humidity of storage and adsorption capacity. Iler [32] constituted that silica gels need a specific ratio of SiOH groups to adsorb H_2O molecules on the surface. This mechanism can be transferred to the adsorption mechanism of SO_2 on silica gels. A dry atmosphere during storage after regeneration of silica gels led to less free silanol groups on the surface of silica gels which are required for gas adsorption. However, an atmosphere with a too high relative humidity accompanies with a saturation of the silica gels surface with H_2O molecules on the silanol groups. Therefore, the silanol groups are no longer available for SO_2 adsorption. Overall, a specific concentration of H_2O molecules in the atmosphere is needed to rehydrate the Si–O–Si surface of silica gels with SiOH bonds and to ensure the SO_2 adsorption.

In Fig. 14, the levels of regeneration of silica gels $V2_{reg.}$, $V3_{reg.}$ and $V4_{reg.}$ regarding dynamic breakthrough capacity (c/c_0 = 0.1) and breakthrough time (c/c_0 = 0,1) are shown. Silica gel $V2_{reg.}$ exhibited the highest level of regeneration of 100 % dynamic adsorption capacity and 100 % breakthrough time. Silica gel $V3_{reg.}$ achieved a level of regeneration that was 67 % regarding the dynamic breakthrough capacity and 84 % regarding the breakthrough time. Silica gel $V4_{reg.}$ attained the smallest level of regeneration with 45 % regarding the dynamic breakthrough capacity and 47 % regarding the breakthrough time. A noteworthy destruction of the pore surface and geometry of the silica gels after thermal regeneration can be excluded since at least $V2_{reg.}$ showed complete capability of regeneration. Furthermore, Iler [32] constituted that the loss

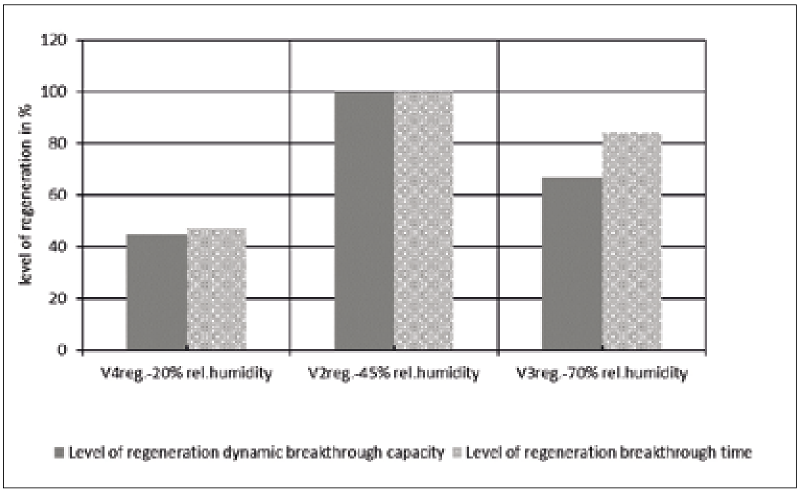

Fig. 14 Level of regeneration of the breakthrough time and dynamic breakthrough capacity of silica gels $V2_{reg.}$, $V3_{reg.}$, and $V4_{reg.}$

of adsorption capacity can also be reasoned by dehydration even at temperatures where the loss of surface through sintering does not occur. From these results can be concluded that the relative humidity seemed to have a larger impact on adsorption of regenerated silica gels than the grain size, since $V2_{reg.}$ with 45 % relative humidity and despite a coarse grain size of 2 mm led to the highest level of regeneration.

4 Conclusions

In this study, the adsorption performance and the breakthrough behaviour regarding SO_2 rich gases as well as the regeneration of silica gels were investigated. Firstly, the influence of different grain sizes on the adsorption of SO_2 and secondly the ability of regeneration regarding different grain size and relative humidity of storing the silica gel were examined.

It was found that the breakthrough time as well as the dynamic adsorption capacity can be increased with decreasing grain size. Therefore, silica gels with a coarse grain size of 2 mm exhibited the smallest breakthrough time and adsorption capacity compared to silica gels with 1 mm fine grains. Small grains lead to shortened diffusion path length without a high mass transfer resistance within the adsorbent particles [28–30] and contributed to larger pressures over the adsorbent than coarse grains. The best silica gel achieved 25 % of dynamic load capacity and 72 % of the breakthrough time compared to standard HOK medium.

Complete regeneration of silica gel was possible with the highest level of regeneration of 100 % adsorption capacity and 100 % breakthrough behaviour. Dependent on the grain size and relative humidity of storage of silica gels, a coarse grain and medium relative humidity of 45 % was favourable for a complete regeneration.

A complete regeneration of adsorbents is economic (conversion, transport, waste removal) and safety-related interesting since conventional carbonaceous adsorbents such as HOK medium or active coke are not regenerated in the industry. For a favourable regeneration, an exorbitant effort is necessary such as regeneration temperatures up to 850 °C [20, 41]. Further disadvantages of thermal regeneration of carbonaceous materials are the loss of carbon and the treatment of exhaust gases [41, 42].

In further investigations, especially the grain size distribution for optimal adsorption behaviour should be investigated and the best pre-treatment should be found to generate an economic important regeneration. In this relation, lower adsorption capacities and breakthrough times can be accepted if multiple regenerations are possible.

Acknowledgements

The authors are grateful to Gert Schmidt for the scanning electron microscopy measurements, to Carolin Ludewig for conducting differential scanning calorimetry measurements and to Ursula Querner for mercury porosimetry, from the institute of Ceramic, Glass and Construction Materials.

References

[1] Kisamori, S.; Kawano, S.; Mochida, I.: SO_2, NOx Removal at ambient Temperatures using activated carbon fibers. Preprints of papers. Amer. Chem. Soc. Division Fuel Chemistry **38** (1993) 421–421

[2] Piechota, R.; Gillmann, P.; Görner, K.: Rauchgasreinigung bei der Verbrennung von Biomasse auf einem wassergekühlten Rost in kleinen dezentralen Anlagen. DGMK-Fachbereichstagung Energetische Nutzung von Biomassen, 2006

[3] Nethe, L.P.: Der Einsatz von Sorbentien im gesamten System von Abgasreinigungsanlagen. Tagung Trockene Abgasreinigung, 2005

[4] Liberti, A.; Brocoo, D.; Possanzini, M.: Adsorption and oxidation of sulfur dioxide on particles. Atmospheric Environment **12** (1978) 255–261

[5] DeBarr, J.A.; Lizzio, A.A.; Daley, M.A.: Adsorption of SO_2 on bituminous coal char and activated carbon fiber. Energy & Fuels **11** (1997) 267–71

[6] Daley, M.A.; et al.: Adsorption of SO_2 onto oxidized and heat-treated activated carbon fibers (ACFs). Carbon **35** (1997) 411–417

[7] Rodriguez-Mirasol, J.; Cordero, T.; Rodriguez J.: Effect of oxygen on the adsorption of SO_2 on activated carbon. Extended Abstracts of 23rd Biennal Conf. on Carbon. College Park, (1997)

[8] Kisamori, S.; et al.: Oxidative removal of SO_2 and recovery of H_2SO_4 over poly(acrylonitrile)-based active carbon fiber. Energy & Fuels **8** (1994) 1337–1340

[9] Krzack, S.: Rohstoffliche und verfahrenstechnische Einflußfaktoren für die Aktivkoksherstellung aus Braunkohlen. Freiberger Forschungshefte A829 (1997)

[10] Heschel, W.; Klose, E.; Krzack, S.: Eigenschaften, Anwendungsbereiche und Herstellungsmöglichkeiten von Kohlenstoffadsorbentien. Freiberger Forschungshefte A829 (1993) 9–20

[11] Krzack, S.; Heschel, W.; Liebscher, R.: Einsatz von Braunkohlenaktivkoks zur Reinigung schadstoffhaltiger Abgase aus Produktionsanlagen der Nichteisenmetallurgie. Freiberger Forschungshefte A829 (1993) 51–60

[12] Cole, R.; Shulman, H.L.: Adsorbing sulfur dioxide on dry ion exchange resins for reducing air pollution. Industrial and Engin. Chemistry **52** (1960) 859–860

[13] Sirkecioğlu, A.; Altav, Y.; Erdem-Şenatalar, A.: Adsorption of H_2S and SO_2 on Bigadiç Clinoptilolite. Separation Sci. and Technol. **30** (1995) 2747–2762

[14] Tantet, J.; Eić, M.; Desai, R.: Breakthrough study of the adsorption and separation of sulfur dioxide from wet gas using hydrophobic zeolites. Gas Separation & Purification **9** (1995) 213–220

[15] Belyakova, L.D.; et al.: Amine-modified silicas: Thermal stability and adsorption of gases. Russian Chem. Bull. **38** (1989) 885–891

[16] Thornsberry, W.L.: Isothermal gas chromatographic separation of carbon dioxide, carbon oxysulfide, hydrogen sulfide, carbon disulfide and sulfur dioxide. Analytical Chemistry **43** (1971) 452–453

[17] Ahmed, M.S; Attia, Y.A.: Multi-metal oxide aerogel for capture of pollution gases from air. Appl. Thermal Engin. **18** (1998) 787–797

[18] Zhao, Y.; et al.: Desulfurization Performance of Ether-Functionalized Imidazolium-Based Ionic Liquids Supported on Porous Silica Gel. Energy Fuels **29** (2015) 1941–1945

[19] Tseng, H.-H.; Wey, M.-Y.: Study of SO_2 adsorption and thermal regeneration over activated carbon-supported copper oxide catalysts. Carbon **42** (2004) 2269–2278

[20] Klinski, S.: Studie: Einspeisung von Biogas in das Erdgasnetz, 2006

[21] Fischer, M.E.: Biogas purification: H_2S removal using biofiltration. Master thesis, University of Waterloo, Waterloo, Ontario, Canada 2010

[22] Chou T.-C.; et al.: Selective removal of H_2S from biogas by a packed silica gel adsorber tower. Biotechnol. Progress **2** (1986) 203–209

[23] Klenert, F.; Fruhstorfer, J.; Aneziris, C.G.: Investigation of transmittance and thermal conductivity properties of silica gels for application as transparent heat insulation materials. J. of Sol-Gel Sci. and Technol. **77** (2015) 315–324

[24] Klenert, F.; et al.: Microstructure and transmittance of silica gels for application as transparent heat insulation materials. J. of Sol-Gel Sci. and Technol. **75** (2015) 602–616

[25] Schießl, C.: Thermische Analyse: Möglichkeiten zur Untersuchung von dentalen Kunststoffen, PhD thesis, Universität Regensburg, Regensburg 2008

[26] Sonnenburg, A.: Strömungssimulation in der Umwelttechnlogie: Effiziente Versuchsplanung mit CFD (Computational Fluid Dynamics). Hessisches Ministerium für Wirtschaft, Verkehr und Landesentwicklung, Wiesbaden 2009

[27] Klöker, M.; et al.: CFD-gestützte Untersuchungen von Hydrodynamik und Stofftransport in Katalysatorschüttungen. Chemie Ingenieur Technik **76** (2004) 236–242

[28] Karau, A.; et al.: The influence of particle size distribution and operating conditions on the adsorption performance in fluidized beds. Biotechnol. and Bioengin. **55** (1997) 54–64

[29] Yean, S.; et al.: Effect of magnetite particle size on adsorption and desorption of arsenite and arsenate. J. of Mater. Research **20** (2005) 3255–3264

[30] Rasmuson, A.: The effect of particles of variable size, shape and properties on the dynamics of fixed beds. Chem. Engin. Sci. **40** (1985) 621–629

[31] Clarkson, C.R.; Bustin, R.M.: The effect of pore structure and gas pressure upon the transport properties of coal: a laboratory and modeling study. 1. Isotherms and pore volume distributions. Fuel **78** (1999) 1333–1344

[32] Iler, R.K.: The Chemistry of Silica: Solubility, Polymerization, Colloid and Surface Properties and Biochemistry. New York 1979

[33] Tseng, H.-H.; et al.: Catalytic removal of SO_2, NO and HCl from incineration flue gas over activated carbon-supported metal oxides. Carbon **41** (2003) 1079–1085

[34] Kast, W.: Adsorption aus der Gasphase: Ingenieurwissenschaftliche Grundlagen und technische Verfahren. Weinheim 1988

[35] Brinker, C.J.; Scherer, G.W.: Sol-gel science: The physics and chemistry of sol-gel processing. Boston 1990

[36] Pramanik, A.; et al.: A mechanistic study of the initial stage of the sintering of sol-gel derived silica nanoparticles. Int. J. of Modern Engin. Res. **3** (2013) 1066–1070

[37] Tsai, W.T.; Lai, C.W.; Hsien, K.J.: Effect of particle size of activated clay on the adsorption of paraquat from aqueous solution. J. of Colloid and Interface Sci. **263** (2003) 29–34

[38] Mehlhorn, T.; Gerbeth, A.; Gemende, B.: Adsorptive Schwefelwasserstoffentfernung aus Biogas-Einfluss von Gasfeuchte und Sauerstoffgehalt auf den Adsorptionsprozess. Intensive Programme "Renewable Energy Sources", (2011) 6–10

[39] Lincke, M.; Klöden, B.; Faßauer, B.: Entwicklung eines neuartigen energie- und rohstoffeffizienten Entschwefelungssystems für die Erzeugung von Bio-Erdgas: Schlussbericht zum Forschungsvorhaben, 2014

[40] Ramesohl, S.; et al.: Analyse und Bewertung der Nutzungsmöglichkeiten von Biomasse: Band 3: Biomassevergasung, Technologien und Kosten der Gasaufbereitung und Potenziale der Biogaseinspeisung in Deutschland. Endbericht, 2005

[41] Salvador, F.; Jiménez, C.: A new method for regenerating activated carbon by thermal desorption with liquid water under subcritical conditions. Carbon **34** (1996) 511–516

[42] Lim, J.-L.; Mitsumasa, O.: Regeneration of granular activated carbon using ultrasound. Ultrasonics Sonochem. **12** (2005) 277–282